
Appendix VIII

Climate Change Sensitivity Study of California Hydrology

Norman L. Miller and Kathy E. Bashford
California Water Resources Research and Applications Center
LBNL, University of California
Berkeley, California

and

Eric Strem
National Oceanic and Atmospheric Administration
National Weather Service
California Nevada River Forecast Center
Sacramento, California

Contents

List of Figures	v
List of Tables	vii
Abstract	1
1 Introduction	1
2 Approach	2
2.1 Incremental Perturbations	5
2.2 Scenario Perturbations	6
3 Results	9
3.1 Temperature	9
3.2 Precipitation	9
4 Summary and Conclusions	21
5 Future Research	22
Acknowledgments	22
References	23
Attachments	
A Temperature Shifts	A-1
B Precipitation Ratios	B-1
C Incrementally Forced Streamflow Sensitivity Values	C-1
D GCM-Forced Streamflow Sensitivity Values	D-1

Figures

1	Location of the six study basins	4
2	California climatological temperature shifts for PCM and HadCM2 averaged over the time periods 2010-2039, 2050-2079, and 2080-2099	7
3	California mean-area climatological precipitation ratios for PCM and HadCM2 averaged over the time periods 2010-2039, 2050-2079, and 2080-2099	8
4	HadCM2 and PCM temperature shifts imposed on the NWS observed temperatures at the Sacramento, American, and Merced study basins.....	10
5	HadCM2 and PCM precipitation ratios imposed on the NWS observed temperatures at the Sacramento, American, and Merced study basins	11
6	Snow and rain mean annual depth for the lower and upper subbasins for each climate baseline, 2010-2025, 2050-2079, and 2080-2099	12
7	Ratio of climate change to baseline mean-monthly SWE for each basin	13
8	Ratio of climate change to baseline mean-monthly snowmelt for each basin	15
9	Streamflow monthly climatologies based on the HadCM2 and the PCM	17
10	Streamflow monthly climatologies based on the specified incremental changes	18
11	The cumulative daily streamflow for each basin	19
12	Exceedence probabilities of the peak daily flow for each year for each climate change scenario	20
13	Exceedence probabilities of the peak daily flow for the specified temperature and precipitation incremental climate change.....	21

Tables

1	Basin area, stream gauge coordinates, percent subbasin area, and elevation.....	4
2	The six specified incremental temperature shifts and precipitation ratios	5
3	Proportion of January 6 h timesteps below freezing for each upper basin for projected climatological periods 2025, 2065, and 2090.....	14

Abstract

Recent reports based on climate change scenarios have suggested that California will be subjected to increased wintertime and decreased summertime streamflow. Because of the uncertainty of projecting future climate, we applied a range of potential climatological future temperature shifts and precipitation ratios to the Sacramento Soil Moisture Accounting Model and the Anderson Snow Model to determine hydrologic sensitivities. Two general circulation model (GCM) projections were used in this analysis: one that is warm and wet (Hadley Climate Center HadCM2 run 1) and one that is cool and dry (PCM run B06.06), relative to the GCM projections that were part of the Third Assessment Report of the Intergovernmental Panel on Climate Change. We used an additional set of specified incremental temperature shifts (1.5°C, 3.0°C, and 5.0°C) and precipitation ratios (1.00, 1.09, 1.18, and 1.30) as input to the snow and soil moisture accounting models. Calculations were performed for a set of California river basins that extend from the coastal mountains and Sierra Nevada northern region to the southern Sierra Nevada region. Results from this study indicate that for all cases, a larger proportion of the streamflow volume will occur earlier in the year. The amount and timing are dependent on the characteristics of each basin, particularly the elevation of the freezing line. The hydrologic response varies for each scenario, and the resulting solution set provides bounds to the range of possible change in streamflow, snowmelt, and snow water equivalent, and the change in the magnitude of annual high flow days.

1. Introduction

The Intergovernmental Panel on Climate Change (IPCC) Third Assessment Report (Houghton et al., 2001) and the U.S. Global Climate Change Research Program Report of the Water Sector (Water Sector Assessment Team, 2000) summarize potential consequences of global warming. The IPCC reports that climate model projections with a transient 1% annual increase in greenhouse gas emissions show an increase in the global mean near-surface air temperature by 1.4°C to 5.8°C, with a 95% probability interval of 1.7°C to 4.9°C by 2100 (Wigley and Raper, 2001). Both reports indicate that likely changes during the 21st century include higher maximum and minimum temperatures with a decreasing diurnal range over U.S. land areas, more intense precipitation events, increased summer continental drying, and increased risk of drought. To assess the impacts on water resources, hydrologic simulations based on climate model projections and specified incremental temperature and precipitation changes that bracket the range of possible outcomes are necessary.

A number of investigations of California hydrologic response have focused on changes in streamflow volumes resulting from climate change (e.g., Revelle and Waggoner, 1983; Gleick, 1987; Lettenmaier and Gan, 1990; Jeton et al., 1996; Miller et al., 1999; Wilby and Dettinger, 2000; Knowles and Cayan, 2001). Using historical data, Revelle and Waggoner (1983) developed regression models to estimate the sensitivity of streamflow in major basins to climate change. Gleick (1987) used a modified upper and lower basin water budget model (Thornwaite and Mather, 1948) for the Sacramento drainage directly forced by precipitation and temperature output from three GCMs. Lettenmaier and Gan (1990) used precipitation and temperature from three general circulation model (GCM) scenarios to force process-based basin-scale water budget models (Anderson, 1973; Burnash et al., 1973) with three to five elevation-band-defined sub-basins at four basins (North Fork American, Merced, McCloud, and Thomes Creek) in the Sacramento-San Joaquin drainage. Jeton et al. (1996) ran a distributed parameter precipitation runoff model (Leavesley et al., 1983) to evaluate the North Fork American and East Fork Carson rivers using specified incremental temperature and precipitation as uniform climate change scenarios. Miller et al. (1999) dynamically downscaled a GCM projection via a regional climate model and used the output as forcing to process-based hydrologic models (Beven and Kirkby, 1979; Leavesley et al., 1983) in the North Fork American River and the north coastal Russian River. Knowles and Cayan (2001) used historical precipitation and a single GCM projection of temperature that was statistically interpolated to a 4 km resolution as input forcing to a modified version of the Burnash et al. (1973) soil moisture accounting model (Knowles, 2000) for the entire Sacramento-San Joaquin drainage.

In general, each of these studies suggested that Sierra Nevada snowmelt-driven streamflows are likely to peak earlier in the season under global warming because of increased atmospheric greenhouse gas (GHG) concentrations. A key finding of these studies is that the greatest influences on streamflow sensitivity to climate change are the basin elevation and the location of the freezing line. To further understand the likelihood of potential shifts in the timing and magnitude of California streamflow and related hydrologic response, we analyzed six major watersheds forced by two end-member GCM projections and by specified incremental temperature (shifts) and precipitation (ratios) changes.

2. Approach

This study focused on determining the range of the effects of projected climate change scenarios for assessing California water resources. Streamflow sensitivities for the watersheds studied were related to a larger set of watersheds representing the entire Sacramento-San Joaquin drainage and were applied to water demand and allocation simulations.

Streamflow simulations in this study are based on the application of the National Weather Service River Forecast System (NWSRFS) Sacramento Soil Moisture Accounting (SAC-SMA) Model (Burnash et al., 1973) coupled to the snow accumulation and ablation Anderson Snow Model (Anderson, 1973). The SAC-SMA has two upper zone storage compartments (free and tension) and three lower zone storage compartments (free primary, free secondary, and tension). Tension zone storage is depleted only by evapotranspiration processes; free zone water drains out as interflow and baseflow. The SAC-SMA was chosen primarily because it depends on only two variables, precipitation and temperature, and because it is the operational model of the NWS. It has been used in previous climate change sensitivity studies (Lettenmaier and Gan, 1990; Miller et al., 2000) with an assumption of geomorphologic stream channel stationarity. Assuming fixed channel geometry requires that climate change simulations be based on perturbations about the historical data period for which the calibration was performed and verified (Lettenmaier and Gan, 1990). Historical temperature and precipitation time series for 30 years (1963-1992) are sufficiently long for a representative climatology and are available at 6 h timesteps for each basin. The snow-producing basins were delineated into upper and lower basins with separate input forcing to account for the elevation, land surface characteristics, and climate differences.

Six representative headwater basins (Smith River at Jed Smith State Park, Sacramento River at Delta, Feather River at Oroville Dam, American River at North Fork Dam, Merced River at Pohono Bridge, and Kings River at Pine Flat Dam) with natural flow were selected for analysis in this study (Figure 1). Table 1 shows the basin size, location, percent area, and centroid of each upper and lower sub-basin. The Smith is a very wet coastal basin that does not significantly accumulate seasonal snowpack. The Sacramento is a mountainous northern California basin with a small amount of seasonal snow accumulation. The Sacramento provides streamflow for the north and northwest drainage region into the Central Valley. The Feather and the Kings represent the northernmost and southernmost Sierra Nevada basins for this study, and the Kings and Merced are the highest elevation basins. The American is a fairly low elevation Sierra Nevada basin, but has frequently exceeded flood stage, resulting in substantial financial losses. This set of study basins provides sufficient information for a spatial estimate of the overall response of California's water supply (excluding the Colorado River) and will help indicate the potential range of impacts.

Historical precipitation and temperature input forcing to the hydrologic models is based on the archived NWS 6 hour mean area precipitation (MAP) and mean area temperature (MAT) for each upper and lower basin. The NWS also provided historical daily streamflow data for the stream gauges at the outlet of each of the six basins.



Figure 1. Location of the six study basins

Table 1. Basin area, stream gauge coordinates, percent subbasin area, and elevation

	Smith	Sacramento	Feather	American	Merced	Kings
Area, km ²	1,706	1,181	9,989	950	891	4,292
Gauge latitude	41° 47' 30"	40° 45' 23"	39° 32' 00"	38° 56' 10"	37° 49' 55"	36° 49' 55"
Gauge longitude	124° 04' 30"	122° 24' 58"	121° 31' 00"	121° 01' 22"	119° 19' 25"	119° 19' 25"
Percent upper	0	27	58	37	89	72
Upper centroid		1798	1768	1896	2591	2743
Lower centroid	722	1036	1280	960	1676	1067

Each basin was calibrated and verified by NOAA’s California Nevada River Forecast Center (CNRFC) using parts of the 6 h and daily 1950 to 1993 precipitation, temperature, and streamflow time series. A 30 year climatological verification for the 1963-1992 period using the CNRFC calibration parameters was performed in this study, because it is the most complete and is close to the National Climatic Data Center (NCDC) 1961 to 1990 climatology. Comparison of the observed to simulated climatological streamflow for 1963-1992 period resulted in monthly streamflow correlation coefficients greater than 0.95 for each of the six basins.

2.1 Incremental Perturbations

Streamflow was estimated by imposing six incremental sets of constant temperature shifts ($T_{\text{shift,incr}}$) and precipitation ratios ($P_{\text{ratio,incr}}$) on the historical MAT and MAP time series (Table 2). The selected incremental values cover a broad range of temperature increases, and the precipitation corresponds to no change or the average change in precipitation per change in temperature, representing the mid- and late 21st century GCM projected changes for California climate. Adjusted 6 h temperature and precipitation input data were calculated by uniformly adding the temperature shift, and multiplying by the precipitation ratio, for each temperature and precipitation time series [$T_{\text{incr}}(t) = T(t)_{\text{hist}} + T_{\text{shift,incr}}$; $P_{\text{incr}}(t) = P(t)_{\text{hist}} * P_{\text{ratio,incr}}$]. For each of the six incremental changes, daily streamflow ($Q_{\text{day,incr}}$) was simulated at each of the representative basins. From these daily streamflow outputs, monthly mean-daily streamflow, in cubic meters per second daily (CMSD), was computed for the time period from October 1963 to September 1992. Monthly climatological means were computed as the monthly mean-daily streamflow for each calendar month over the 30 year period ($Q_{\text{month,incr}}$). Monthly means were also calculated for each observed 1963-1992 streamflow time series to provide historical mean-monthly baseline climatologies ($Q_{\text{month,hist}}$).

Table 2. The six specified incremental temperature shifts and precipitation ratios

Temperature shift (degrees C)	Precipitation ratio
1.5	1.00
1.5	1.09
3.0	1.00
3.0	1.18
5.0	1.00
5.0	1.30

2.2 Scenario Perturbations

The scenario perturbation studies used a warm, wet GCM climate projection based on the Hadley Centre's HadCM2 run 1 and a cool, dry climate projection based on the National Center for Atmospheric Research (NCAR) PCM run B06.06, relative to the IPCC GCM projected output for California. From these coupled atmosphere-ocean GCM simulations, two 30 year periods (2010-2039 and 2050-2079) and one 20 year period (2080-2099) were used. The GCM data were statistically downscaled and interpolated to a mean-monthly temporal and 10 km spatial resolution using historically derived regression equations based on the PRISM technique (Daley et al., 1999). Monthly temperature shifts and precipitation ratios derived from the mean-area basin climatologies were then imposed on the historical 1963-1992 temperature and precipitation time series as in the incremental studies. The California 10 km resolution temperature shifts (Figure 2) averaged for each climatological period indicate that statewide, the PCM temperature difference increases to about 1.5°C by 2050 and to 2.4°C by 2100. The HadCM2 increases to about 2.4°C by 2050 and to 3.3°C by 2100. The precipitation ratios (Figure 3) indicate that PCM precipitation is reduced to about 0.91 of present precipitation by 2010-2039, 0.86 by 2050-2079, and 0.76 by 2080-2099, while the HadCM2 precipitation ratio increased to about 1.22 by 2010-2039, 1.32 by 2050-2079, and 1.62 by 2080-2099. This coarse climatology indicates the overall spatial variations, but not the seasonal variations of the changes.

GCM-based monthly mean-area precipitation and temperature were determined for each upper and lower sub-basin as the mean of the 10 km gridded temperature and precipitation within the sub-basin. Similarly, a set of basin mean-area historical monthly MAP and MAT time series were derived from the available 10 km derived historical data for 1963-1992. Baseline climatological monthly MAP and MAT values were calculated from these 30 year records.

A ratio (shift) between the monthly basin mean area MAP_{scen} (MAT_{scen}) climatologies for the projected time periods and the monthly baseline historical precipitation (temperature) climatologies was computed. These climate scenario precipitation ratios ($P_{ratio,scen}$) and temperature shifts ($T_{shift,scen}$) were used to adjust the archived NWS observed time series in a similar manner as the constant incremental values, but in this case, monthly adjustments were made. The imposed climate scenario mean-area precipitation and temperature time series were used as input to the hydrologic models as described in the incremental approach.

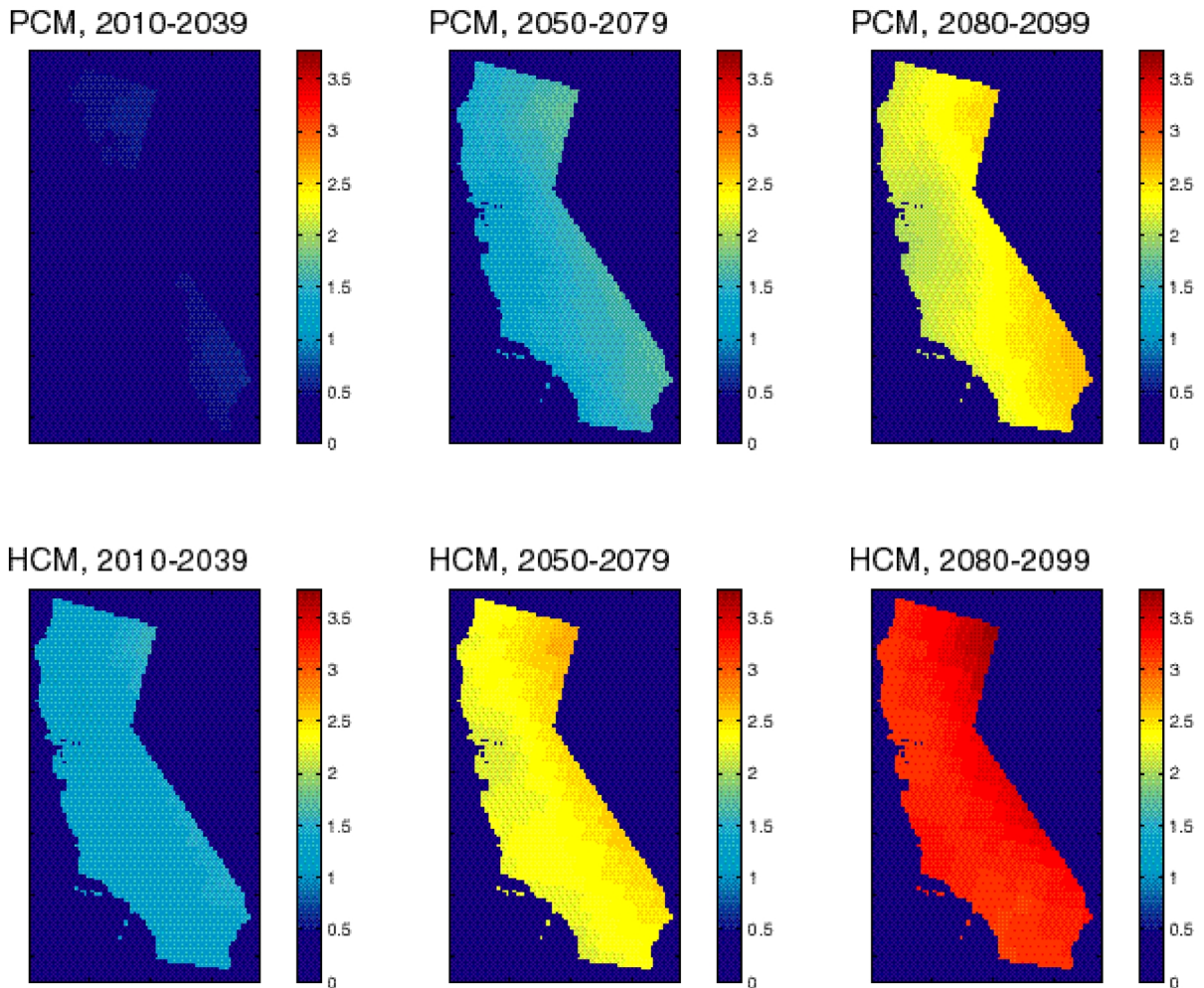


Figure 2. California climatological temperature shifts (degrees C) for PCM and HadCM2 averaged over the time periods 2010-2039, 2050-2079, and 2080-2099

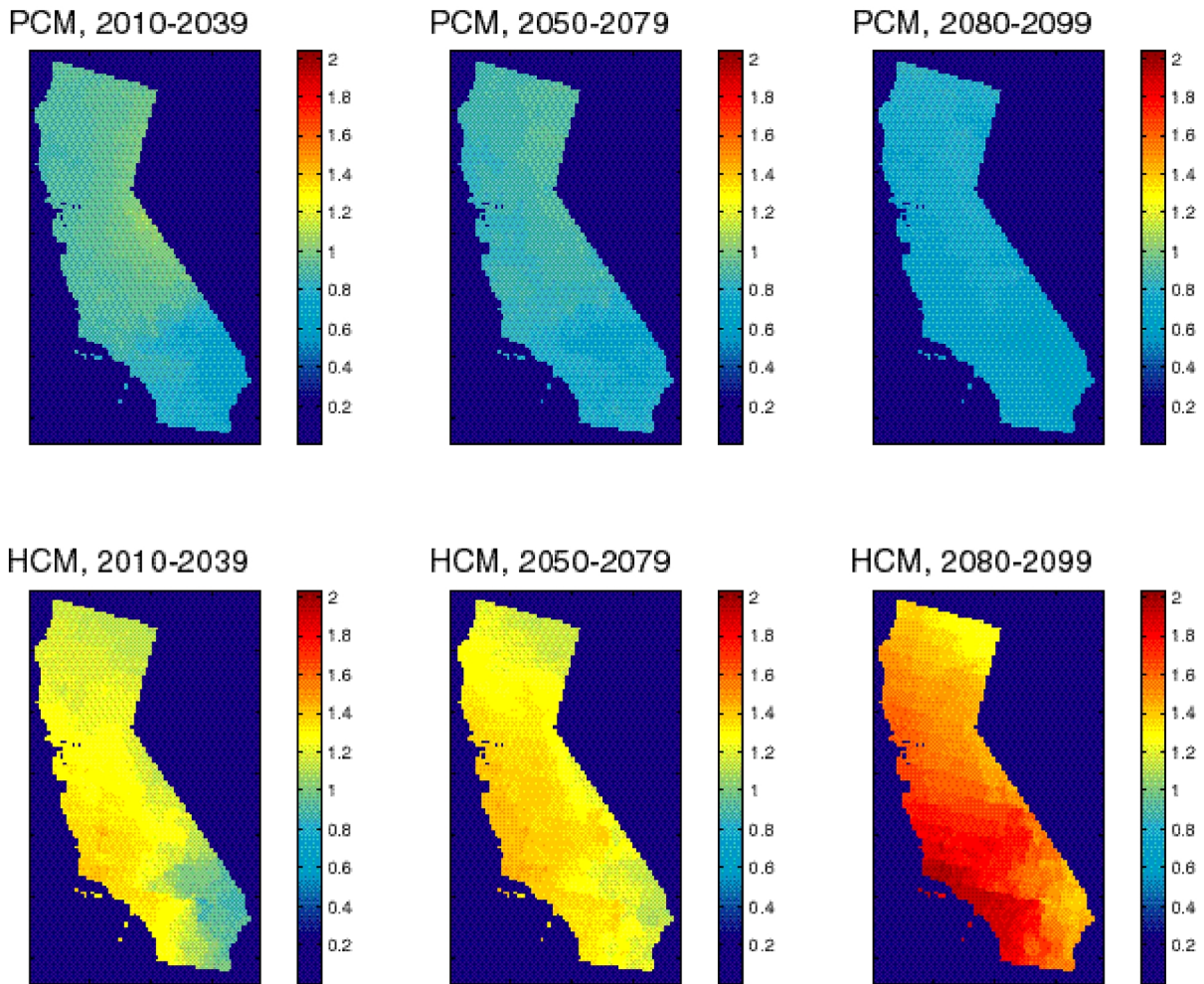


Figure 3. California mean-area climatological precipitation ratios for PCM and HadCM2 averaged over the time periods 2010-2039, 2050-2079, and 2080-2099

3. Results

Analysis of temperature, precipitation, snow-to-rain with elevation, snowmelt, and streamflow was based on the mean monthly climatologies. Shifts in the cumulative streamflow and exceedence probabilities of peak streamflow were based on the perturbation of the daily 30 year time series and annual peakflow.

3.1 Temperature

Figure 4 shows the annual temperature cycle at three of the headwater study basins (Sacramento, American, and Merced) for the two GCM projections (HadCM2 and PCM) superimposed on the NWS observed data. The simulated temperature climatologies generally follow the historical seasonal trends, with quasilinear increases with time. The greatest increases from the baseline are during June to August (JJA) season, and in January, with the largest increase during HadCM2 2080-2099, followed by HadCM2 2050-2079, then PCM 2080-2099. The monthly temperature shift ranges are 0.53°C to 4.70°C for the HadCM2 and -0.14°C to 3.00°C for the PCM (see tables in Attachment A).

The sensitivity of snowmelt to temperature increases depends on how many degrees the baseline temperature is below freezing during these months. The high-elevation upper Merced and Kings basins, where the December to February (DJF) temperatures are several degrees below freezing, are less sensitive to small temperature increases than the upper American basin, where the DJF temperatures are about 1°C below freezing. The increased summertime heating will increase evapotranspiration, reducing soil moisture storage and streamflow.

3.2 Precipitation

Figure 5 shows the mean-monthly precipitation for the same three headwater basins discussed in the previous sections. The simulated future climate mean-monthly precipitation volumes do not follow the historical cycle closely. The warm, wet HadCM2 increases in monthly amounts from November to March, and generally shifts the maximum precipitation by about 1 month later in the year. The PCM total annual precipitation is close to the historical precipitation; however, precipitation decreases from November to December and again during March and April for the 2050-2079 and 2080-2099 mean climates. In January, the 2050-2079 period shows a large increase, whereas the other months show a significant decrease.

The wet HadCM2 projection consistently shows higher ratios than the drier PCM projection. The HadCM2 has a minimum wet season precipitation ratio of 0.89 in December 2010 to 2039 and a maximum of 2.04 times the baseline during February 2080 to 2099. The PCM precipitation

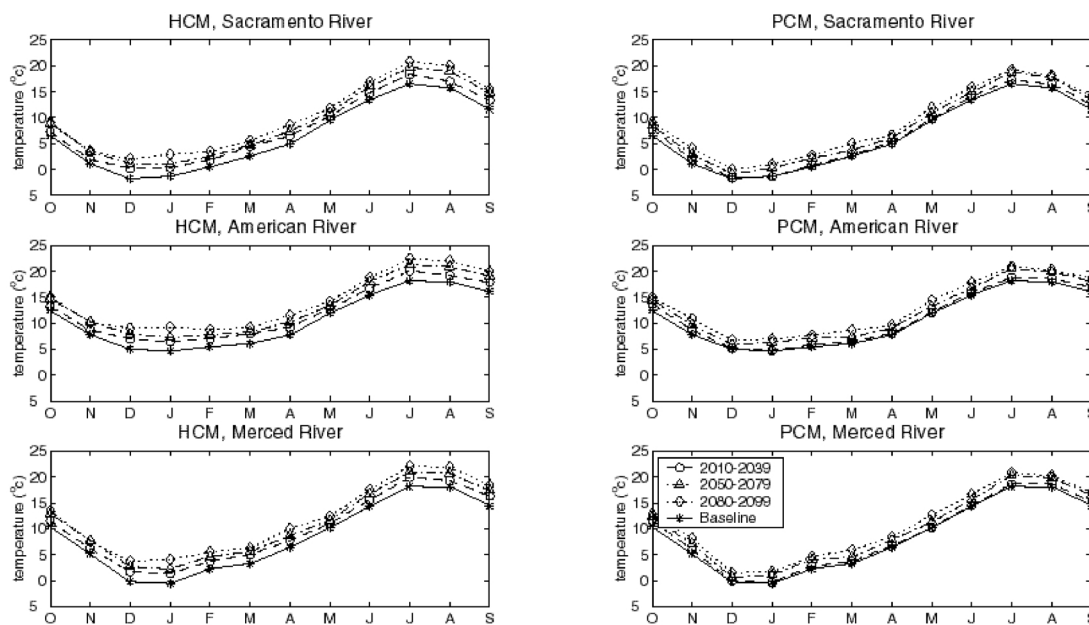


Figure 4. HadCM2 (HCM) and PCM temperature shifts imposed on the NWS observed temperatures at the Sacramento, American, and Merced study basins

ratios have a much smaller range, with a wet season minimum of 0.48 times the baseline in November 2080 to 2099 and a maximum of 1.16 times the baseline in January 2050 to 2079. The range of PCM precipitation ratios is less than the high incremental precipitation ratio (1.3) and shows a decrease in precipitation. The HadCM2 exceeds the high incremental ratio in the Merced and Kings basins for 2050-2079, and in all basins for 2080-2099. The tables in Attachment B present the precipitation ratio values.

3.2.1 Snow-to-rain ratios

The snow-to-rain ratios vary significantly with latitude and most important with the level of the lower and upper basins. In this study, the elevation band partition was based on the historical snow accumulation line. The Anderson Snow Model’s area elevation curve and the snow-to-rain line determine the percentage of the sub-basin’s area that is covered by snow and how that snow-covered area changes over time. This removes the need for a large number of elevation band sub-basins for determining the percent snow and percent rain within each sub-basin area.

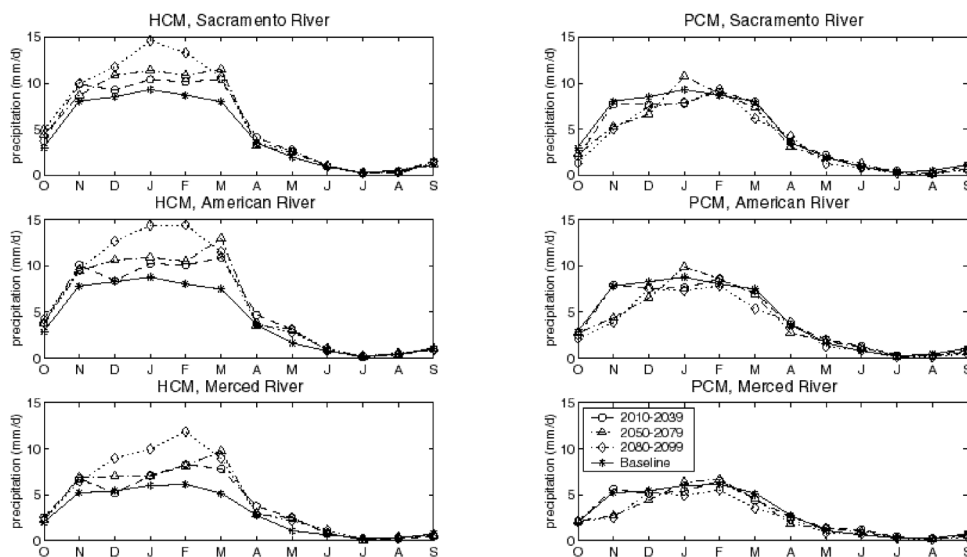


Figure 5. HadCM2 (HCM) and PCM precipitation ratios imposed on the NWS observed temperatures at the Sacramento, American, and Merced study basins

The lower sub-basins typically have minimal to no accumulation and the upper sub-basins have the majority of the accumulated snow. High-elevation sub-basins (e.g., Upper Merced at 2591 m) see higher snow accumulations and later season runoff than do the lower elevation sub-basins (e.g., Upper Sacramento at 1798 m) for the climate change scenarios. The elevation-dependent snow-to-rain ratios shift in amount for each projection (Figure 6). Although the HadCM2 projections show a significant increase in total precipitation, and the PCM projections show reduced precipitation, both cases show a significant reduction of the snow-to-rain ratio.

3.2.2 Snow water equivalent

Figure 7 shows the change relative to the baseline snow water equivalent of the snowpack for the snow-producing upper and lower sub basins. The snow water equivalent (SWE) decreases for most basins, except the very high Kings basin (73% of the basin area is in the upper sub-basin, which has a center of elevation at 2743 m), using the wet and warm HadCM2. The peak snowmelt month similarly shifts earlier for the low-elevation basins and is unchanged for the high ones. For the PCM projections, the snow water equivalent is significantly reduced, and the peak is earlier for all basins by 2080 through 2099. The critical factor is whether the historical temperature is sufficiently below freezing for the snowpack to be unaffected by a small temperature increase.

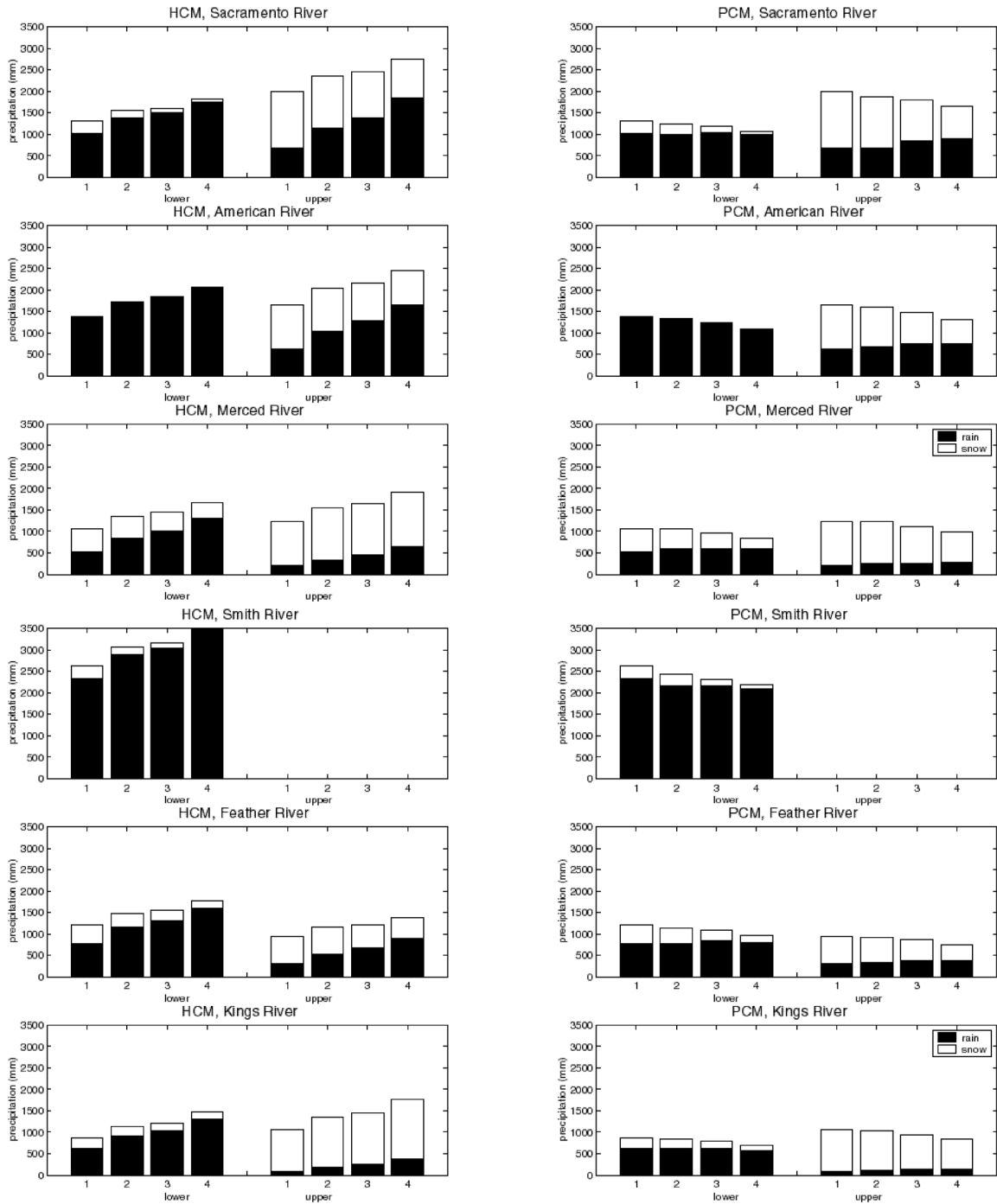


Figure 6. Snow (clear) and rain (solid) mean annual depth for the lower and upper subbasins for (1) each climate baseline, (2) 2010-2025, (3) 2050-2079, and (4) 2080-2099

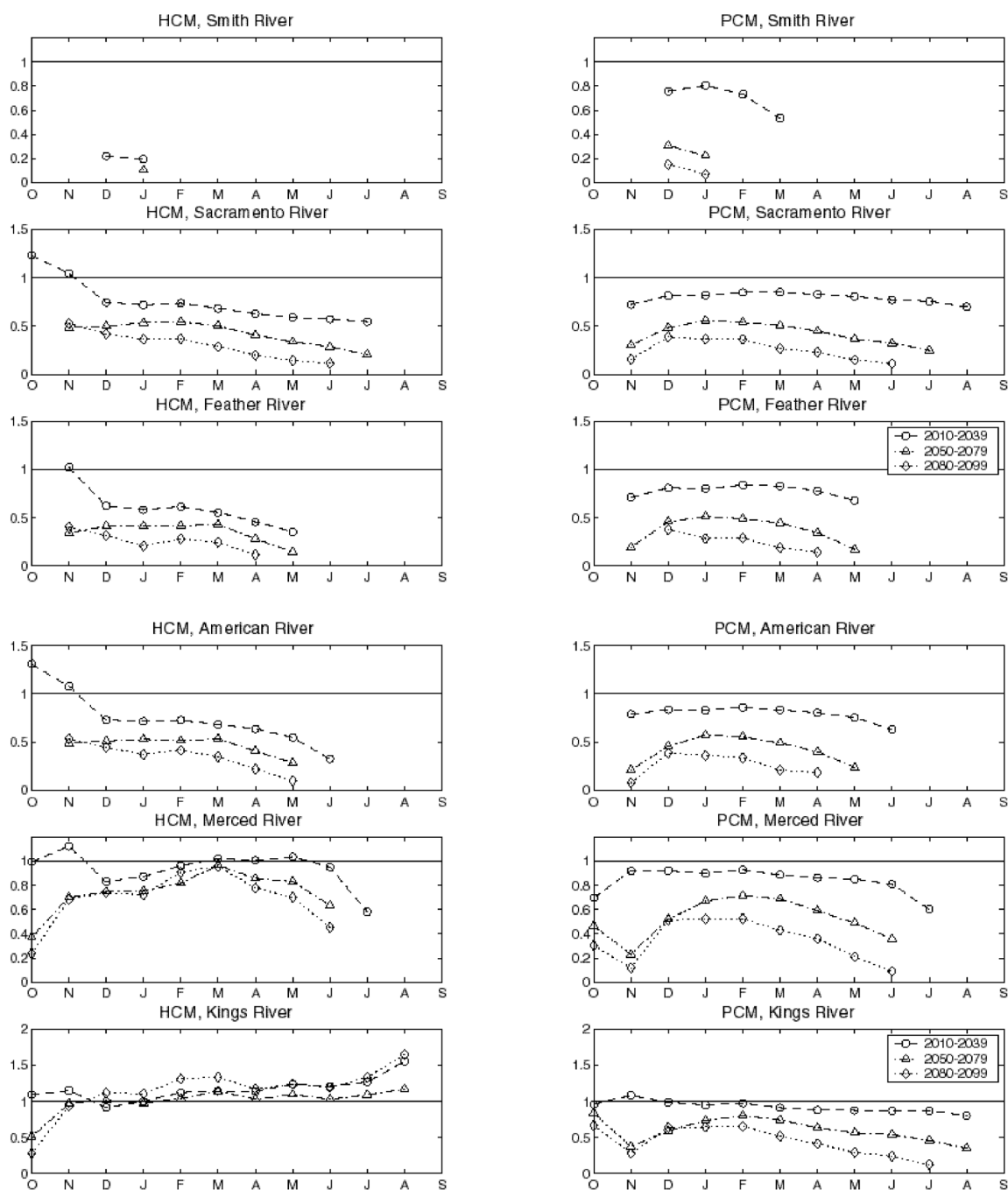


Figure 7. Ratio of climate change to baseline mean-monthly SWE for each basin

Table 3. Proportion of January 6 h timesteps below freezing for each upper basin for projected climatological periods 2025 (2010-2029), 2065 (2050-2079), and 2090 (2080-2099)

	Sacramento	Feather	American	Merced	Kings
Baseline	0.7140	0.6710	0.5634	0.6621	0.7002
H 2025	0.5538	0.5215	0.4368	0.5336	0.5619
P 2025	0.7228	0.6661	0.5556	0.6532	0.6895
H 2065	0.4941	0.4591	0.3782	0.4645	0.5014
P 2065	0.5624	0.5336	0.4470	0.5554	0.5901
H 2090	0.3153	0.3164	0.2478	0.3134	0.3546
P 2090	0.5005	0.4731	0.3989	0.5129	0.5449

In all cases (except the very high-elevation Kings), the SWE decreases as temperature increases. In general, higher elevation basins are less sensitive and do not lose as much winter season snowpack as those with centroid elevations near the freezing line. Table 3 gives the proportion of time (6 h timesteps) for which the upper sub-basins are below freezing during January. The HadCM2 proportion of January that is below freezing decreases by more than 50%; whereas the PCM decreases by about 25%. The large difference is due to the differences in the rate of projected warming.

3.2.3 Snowmelt

Snowmelt and rain represent the liquid water input for evaporation, infiltration, and streamflow response. The increased temperature and precipitation for the HadCM2 simulation yield a consistent early season increase in the liquid water input to the hydrologic system as the projections go from 2010 to 2099. Likewise, the relatively cool and dry PCM projection, with temperatures increasing at a slower rate, results in earlier season snowmelt. The peak timing for each simulation shifts toward earlier in the year as the snow-to-rain ratio decreases. The change in the liquid water amount is more pronounced in the lower elevation basins during the early part of the century and then shifts to the higher elevation basins toward the end of the century, as a result of the proximity of the freezing line to the lower basins. As the freezing line moves to higher elevation, the percentage of area that is melting in the lower basin increases.

An evaluation of the ratio of monthly climate change to baseline snowmelt (Figure 8) shows a large increase for the American, Merced, and Kings basins during DJF and a large decrease during March to May (MJJ) for the HadCM2. A similar, but smaller shift occurs for the cooler and drier PCM.

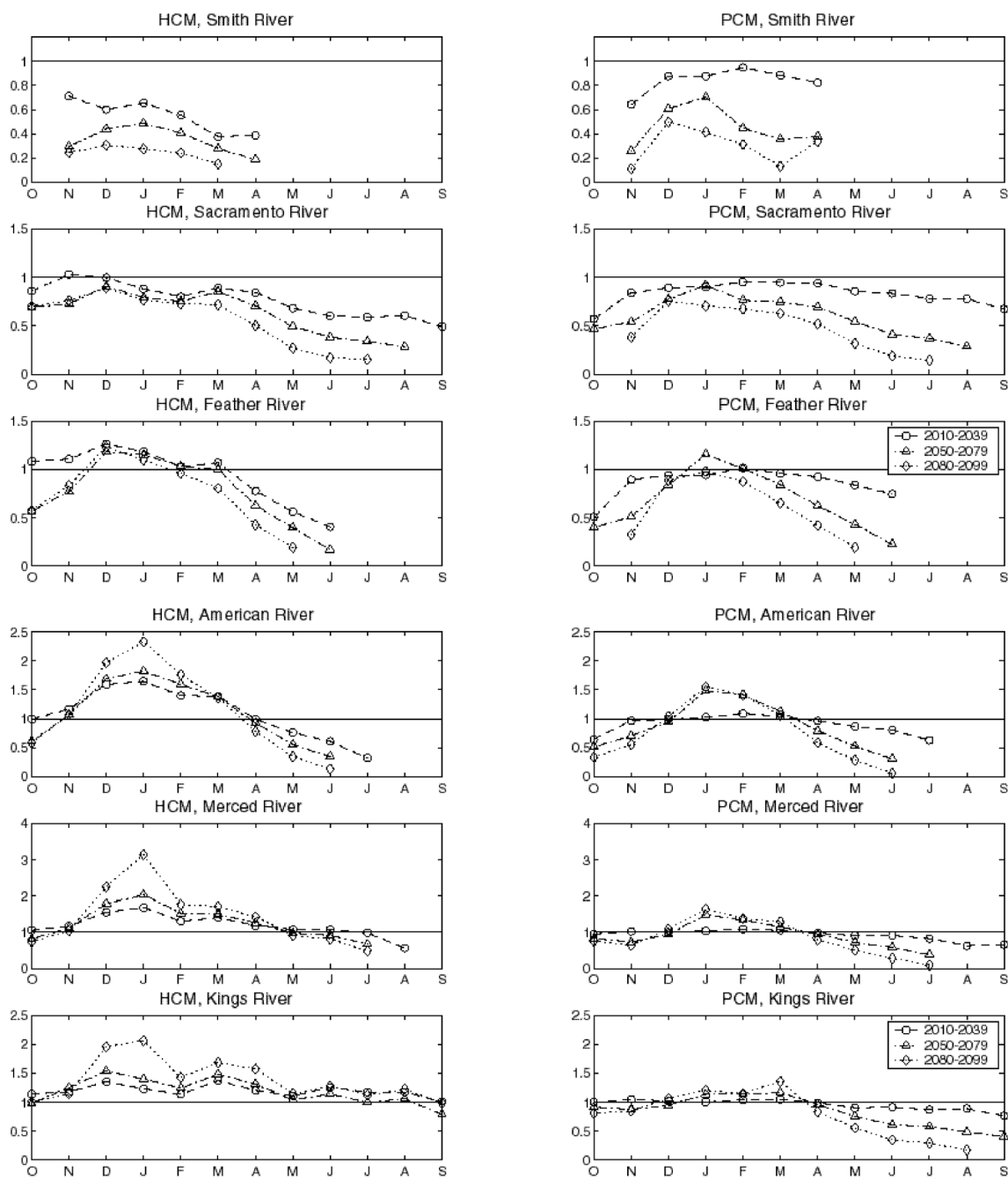


Figure 8. Ratio of climate change to baseline mean-monthly snowmelt for each basin

3.2.4 Streamflow

The nonlinear streamflow response as forced by temperature and precipitation change is sensitive to the characteristics of the basin, particularly the snowline elevation and the local weather pattern. Figure 9 shows the mean-monthly climatological streamflow for the study basins forced by the two GCM-simulated temperature shifts and precipitation ratios imposed on the historical time series. The warm and wet HadCM2-forced streamflow shows large increases in total annual streamflow, increases during the DJF and MAM seasons (for most of the basins), and earlier peakflow timing for the 2080-2099 period. The cool and dry PCM-forced streamflow shows a modest increase in DJF flow volume and decreased JJA streamflow.

The runoff coefficient (streamflow divided by precipitation) increases during November to March and decreases during April to July for the upper sub-basins as forced by both GCM scenarios. This is consistent with the increasing number of days above freezing for each sub-basin.

Figure 10 shows the incrementally uniform shifts in streamflow response. The low-end climate change is represented by 1.5°C with 0% and 9% precipitation increase. The upper end uniform increase is represented by 5°C with 0% and 30% precipitation increase. For the basins studied, a 1.5°C increase is not sufficient for an earlier monthly peakflow. This does, however, show up at 3°C for the Kings, and at 5°C for the other snow-accumulating sub-basins. For all the snow-accumulating basins evaluated, the DJFM monthly streamflow volume increases above the baseline and the MJJA volume decreases below the baseline.

3.2.5 Cumulative streamflow

The cumulative daily streamflow, starting from the beginning of each water year (October 1), is plotted in Figure 11. For both simulations, the day in which 50% of the annual flow has occurred is earlier, as the projected streamflow goes from 2010 to 2100. The HadCM2 is very pronounced with large shifts in both the amount and timing; the PCM shows mainly a shift in timing and reduced magnitude. This is consistent with the PCM precipitation ratio decreasing. The HadCM2 streamflow shifts between 30 and 60 days earlier, and the PCM is less than or about 30 days near 2100.

3.2.6 Exceedence probabilities

Changes in the SWE, coupled with increased wintertime warm precipitation (rain), suggest the increased likelihood of more extreme events such as floods. Ranking each set of 30 year peak annual daily flows and generating probability-of-exceedence plots (Figure 12) indicates that for both the warm and wet HadCM2 and the cool and dry PCM there is a significant increase in the

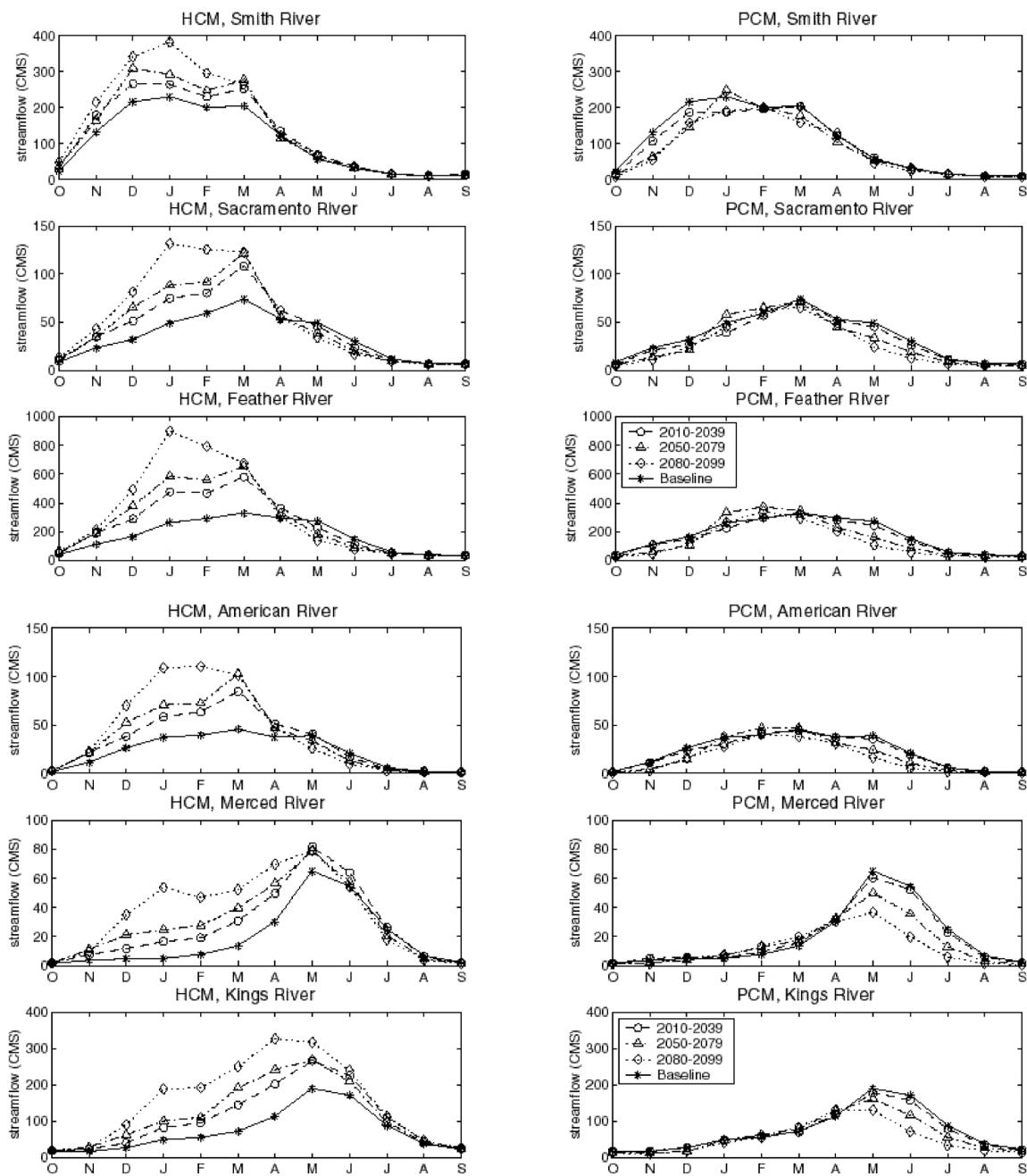


Figure 9. Streamflow monthly climatologies based on the HadCM2 (HCM) and the PCM

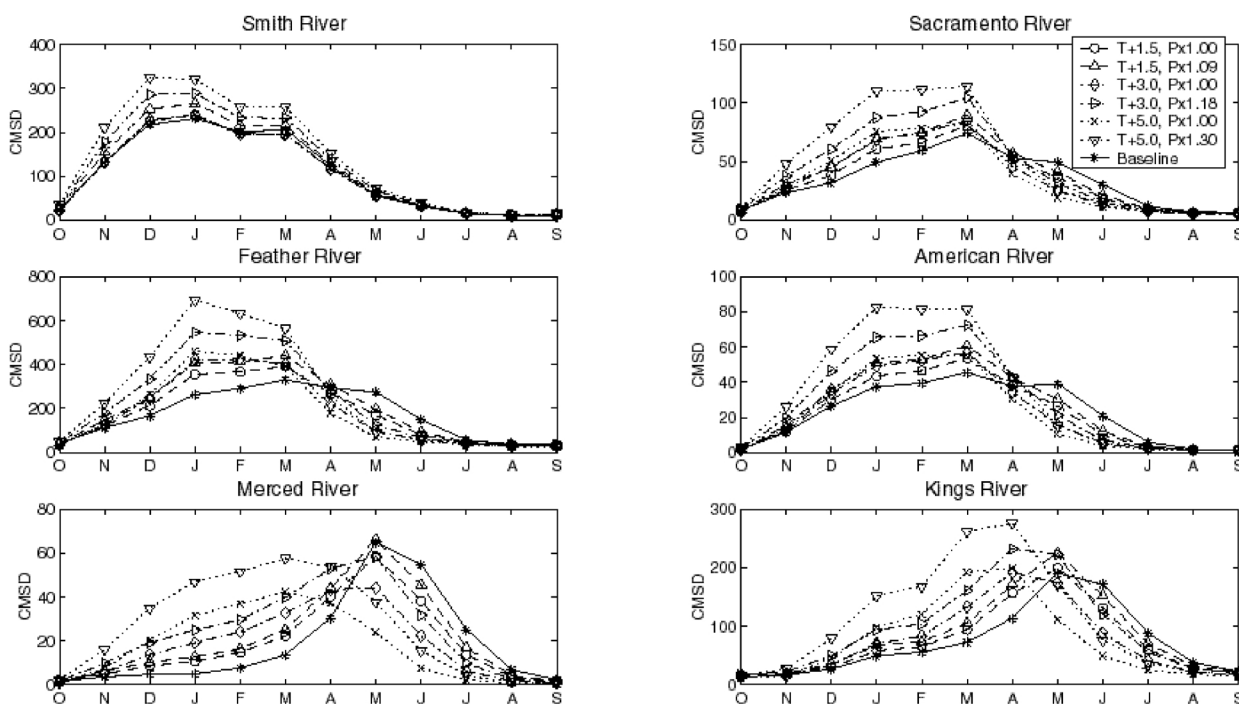


Figure 10. Streamflow monthly climatologies based on the specified incremental changes

likelihood of high-flow days. For each curve shown, the mean annual maximum daily flow is at the 50% exceedence interval. Inspecting this figure points to the very large increase in high-flow occurrence, and a 5% exceedence in high flow for the projected climates that far exceeds current conditions. Figure 13 also shows the consistently large shifts in the 5% exceedence.

3.2.7 Limitations

Determining the impacts of climate change on water resources by evaluating the response of the SAC-SMA to climate change scenarios and incremental changes is a valid approach. The temperature shifts and precipitation ratios imposed on the historical time series constrain the results to perturbations imposed on the historical. This approach removes the variance that indicates extreme events within the climate change time series. However, this is the current impact assessment approach and this study will be useful for applications of water demand and for agro-economic assessments.

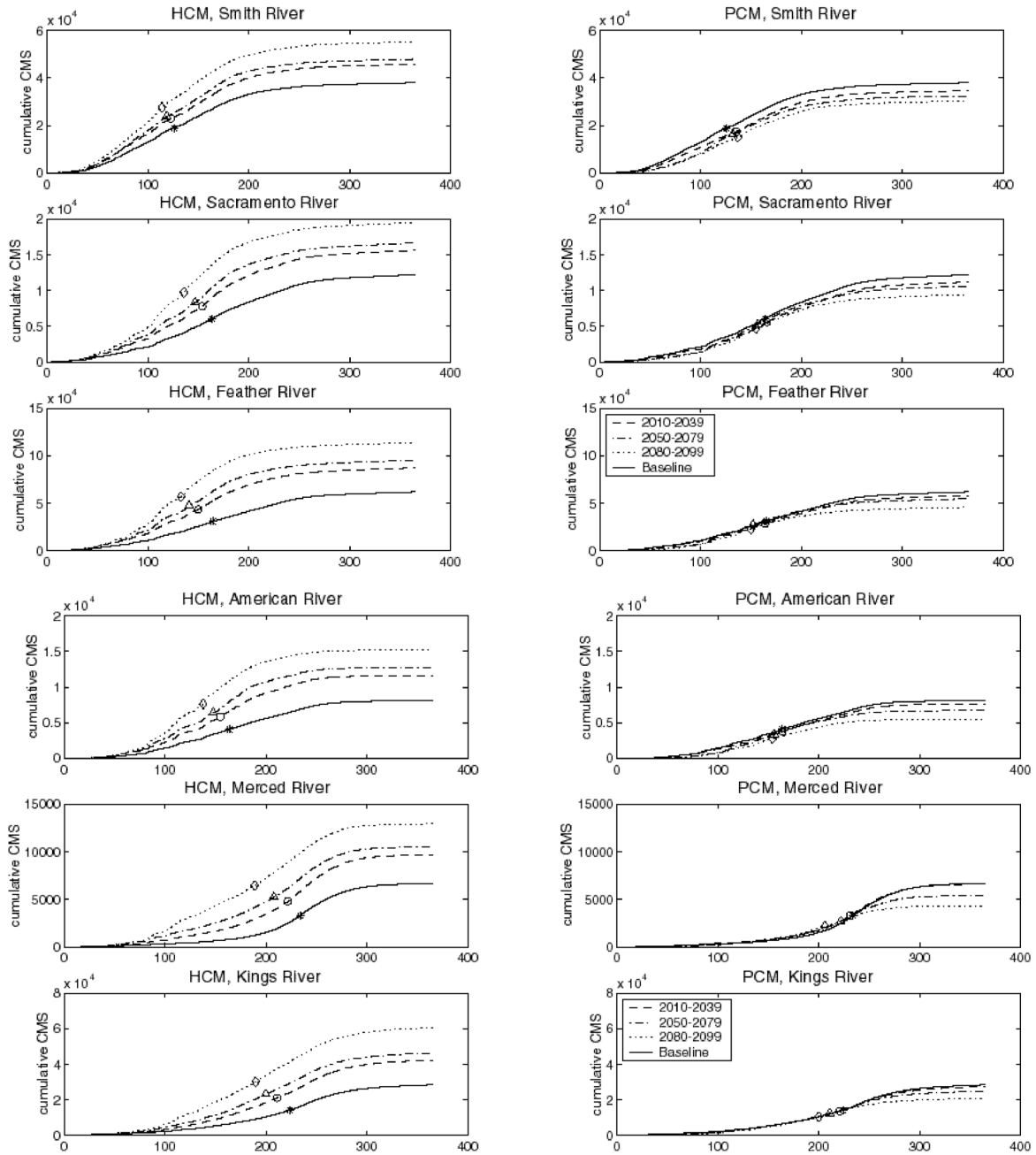


Figure 11. The cumulative daily streamflow for each basin. Day 1 is October 1 and the day in which 50% of the annual flow has occurred is marked with a symbol.

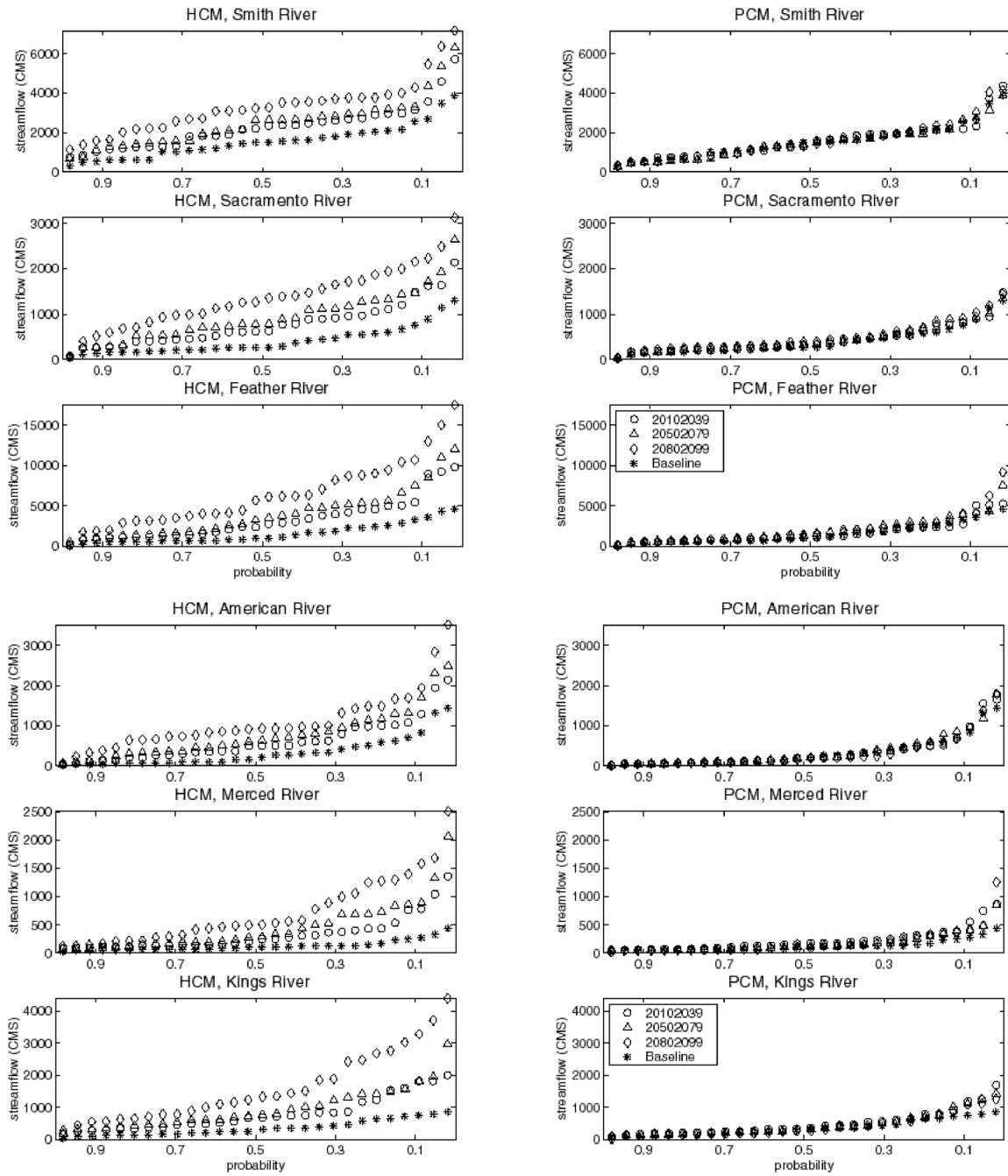


Figure 12. Exceedence probabilities of the peak daily flow for each year for each climate change scenario

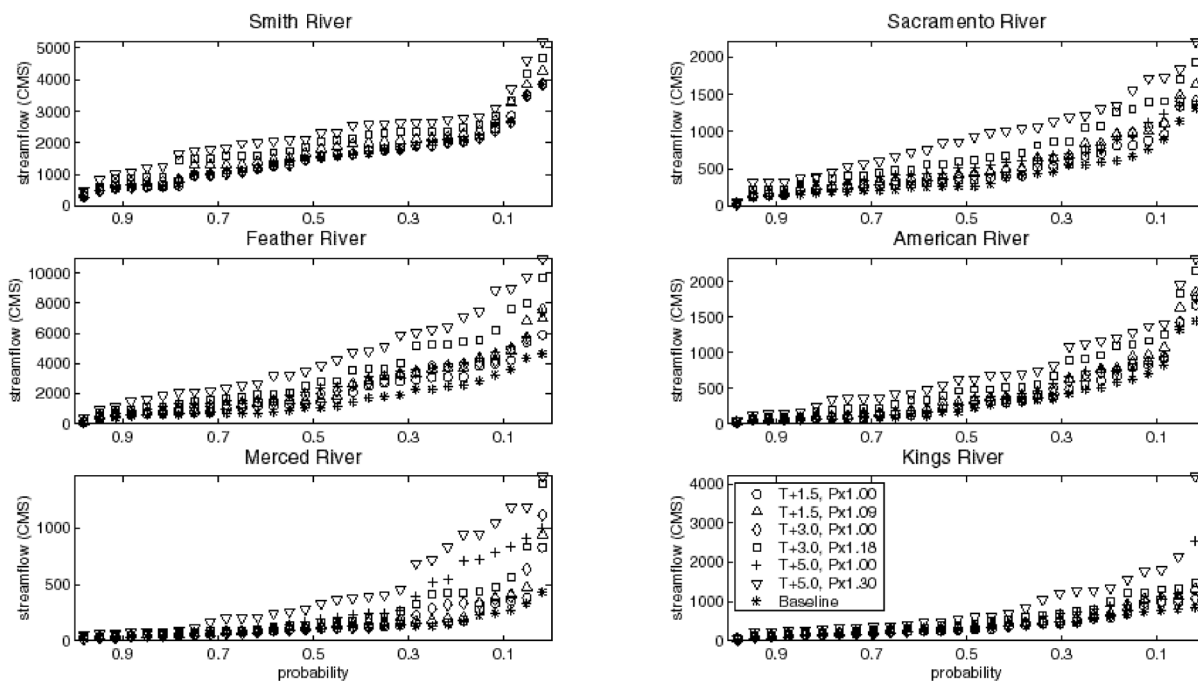


Figure 13. Exceedence probabilities of the peak daily flow for the specified temperature and precipitation incremental climate change

Interpreting the results should remain somewhat qualitative because of the overall uncertainty in model projections. The assumption of fixed land use results in surface characteristics in both the GCMs and the SAC-SMA that do not adequately represent future energy and water budgets. Using the SAC-SMA with a fixed evapotranspiration (ET) demand curve cannot explicitly yield ET climate change response with temperature, which is important during the dry March through August period. This implies that the simulated streamflow is higher than it should be during these periods of evapotranspiration depletion. This effect is not significant during the snow accumulation period and is of less magnitude than GCM uncertainties such as cloud fraction.

4. Summary and Conclusions

For this study, we analyzed California hydrologic response resulting from temperature shifts and precipitation ratios based on two GCM projections and six specified uniform changes. Streamflow and snowmelt timing shifts are discussed here as lower and upper bounds of the set of possible outcomes. For all cases, there are fewer freezing days with climate change than in the present day during the snowpack storage months. More water flows through the system in the winter and less will be available during the dry season. The large shift in the likelihood of high flow days is an important result that appears for all cases considered. The results suggest that the

range of possible climate change responses is attributable to large-scale change and local characteristics. This could be intensified if there are large-scale frequency or intensity changes, or both, in natural low-frequency variations (e.g., the El Niño/Southern Oscillation, the Pacific Decadal Oscillation, and the Arctic Oscillation). Large-scale weather patterns that influence precipitation and runoff timing may dynamically shift, resulting in significantly different local climates.

In this study, monthly changes were superimposed on the historical dataset, so the effects of more intense rainfall events were not represented. The predicted decreasing diurnal temperature ranges (Houghton et al., 2001) were also not represented by this method.

5. Future Research

A number of aspects of future climate simulation analysis studies need to be extended. First, there is a need to further evaluate the GCM results and reduce the model bias. More GCM ensemble members of the most recent simulations are needed. Archived subdaily time series will reduce the amount of statistical interpolation and reduce some errors. Second, dynamic downscaling needs to be incorporated into these studies. A key question is: What scale is of most importance in capturing orographically produced precipitation in California? Certainly GCM resolutions are insufficient, even with the statistical downscaling applied. Another important question is: How many downscaled runs are required and should there be an ensemble of downscaled simulations for each GCM simulation? Third, improving ET as a temperature-dependent derivation and channel routing for capturing the timing more accurately in the SAC-SMA is necessary.

Given these limitations, this study does provide an important and reasonable set of upper and lower bounds of hydrologic response to climate change in California. Climate models will never predict the future, but can yield projections with an uncertainty that can be bracketed. These bracketed solution sets may ultimately give water resource decision makers the type of information needed to safeguard one of our more important natural resources.

Acknowledgments

We thank the NOAA/NWS California Nevada River Forecast Center for collaborating with us on the application of the SAC-SMA and for providing historical streamflow data. We thank NCAR and the Hadley Centre for supplying the Arctic Oscillation GCM output. We also thank Ron Nielson and Chris Daley of Oregon State University for furnishing statistically interpolated 10 km resolution historical and projected precipitation and temperature time series. Sue Kemball-Cook's help mapping the 10 km fields onto the target watersheds is much appreciated.

This project is part of a California Energy Commission (Commission) study on the impacts of climate change in California. The project was supported by Stratus Consulting with funds provided to the Electric Power Research Institute by the Commission and by NASA/Regional Earth Sciences Applications Center Grant NS-2791. Work at the U.S. Department of Energy is under contract number DE-AC03-76F00098.

References

Anderson, E.A. 1973. National Weather Service River Forecast System: Snow Accumulation and Ablation Model. NOAA Technical Memorandum NWS HYDRO-17. National Oceanic and Atmospheric Administration, Boulder, CO.

Beven, K.J. and M.J. Kirby. 1979. A physically based, variable contributing area model of basin hydrology. *Hydrologic Sciences Bulletin* 24:43-69.

Burnash, R.J.C., R.L. Ferral, and R.A. McQuire. 1973. A generalized streamflow simulation system. In *Conceptual Modeling for Digital Computers*. U.S. National Weather Service, Washington, DC.

Daly, C., T.G.F. Kittel, A. McNab, J.A. Royle, W.P. Gibson, T. Parzybok, N. Rosenbloom, G.H. Taylor, and H. Fisher. 1999. Development of a 102-year high resolution climate data set for the conterminous United States. In *Proceedings, 10th Symposium on Global Change Studies, 79th Annual Meeting of the American Meteorological Society, January 10-15, Dallas, TX*, pp. 480-483.

Gleick, P.H. 1987. The development and testing of a water balance model for climate impact assessment: Modeling the Sacramento Basin. *Water Resources Research* 23:1049-1061.

Houghton, J.T., Y. Ding, D.J. Griggs, M. Noguera, P.J. van der Linden, D. Xiaosu, and K. Maskell (eds.). 2001. *Climate Change 2001: The Scientific Basis*. Cambridge University Press, New York.

Jeton, A.E., M.D. Dettinger, and J.L. Smith. 1996. Potential Effects of Climate Change on Streamflow: Eastern and Western Slopes of the Sierra Nevada, California and Nevada. U.S. Geological Survey Water Resources Investigations Report 95-4260. USGS, Washington, DC.

Knowles, N. 2000. Modeling the Hydroclimate of the San Francisco Bay-Delta Estuary and Watershed. PhD Dissertation. Scripps Institution of Oceanography, La Jolla, CA, University of California, San Diego.

Knowles, N. and D.R. Cayan. 2001. Global climate change: Potential effects on the Sacramento-San Joaquin watershed and the San Francisco Estuary. Available at <http://meteora.ucsd.edu/~knowles/papers/Globaland California.pdf>.

Leavesley, G.H., R.W. Litchy, M.M. Troutman, and L.G. Saindon. 1983. Precipitation-Runoff Modeling System User's Manual. U.S. Geological Survey Water Resources Investigations Report 83-4238. USGS, Washington, DC.

Lettenmaier, D.P. and T.Y. Gan. 1990. Hydrologic sensitivities of the Sacramento-San Joaquin River Basin, California, to global warming. *Water Resources Research* 26:69-86.

Miller, N.L., J. Kim, R.K. Hartman, and J. Farrara. 1999. Downscaled climate and streamflow study of the Southwestern United States. *Journal of the American Water Resources Association* 35:1525-1537.

Revelle, R.R. and P.E. Waggoner. 1983. Effects of a carbon dioxide induced climatic change on water supplies in the Western United States. In *Changing Climate*. National Academy of Sciences Press, Washington, DC.

Thornthwaite, C.W. and J.R. Mather. 1948. The water balance. In *Publications in Climatology*. Laboratory of Climatology, Drexel Institute of Technology, Centerton, NJ.

Water Sector Assessment Team. 2000. Water: The Potential Consequences of Climate Variability and Change for the Water Resources of the United States. The Report of the Water Sector Assessment Team of the National Assessment of the Potential Consequences of Climate Variability and Change. Pacific Institute for Studies in Development, Environment, and Security, Oakland, CA.

Wigley, T.M.L. and S.C.B. Raper. 2001. Interpretation of high projections for global-mean warming. *Science* 293:451-454.

Wilby, R.L. and M.D. Dettinger. 2000. Streamflow changes in the Sierra Nevada, California, simulated using statistically downscaled general circulation model output. In *Linking Climate Change to Land Surface Change*, S. McLaren and D. Kniven (eds.). Kluwer Academic Publishers, New York, pp. 99-121.

Appendix VIII — Attachment A

Temperature Shifts

Temperature shifts for upper (gray rows) and lower (clear rows) sub-basins for the six study watersheds are provided. Tables A.1 to A.3 show the representative temperature shifts for the HadCM2 scenario at time periods 2010-2039, 2050-2079, and 2080-2099, respectively. Tables A.4 to A.6 show the representative temperature shifts for the PCM scenario at time periods 2010-2039, 2050-2079, and 2080-2099, respectively.

Table A.1. Temperature shifts HadCM2 2010-2039 (degrees Celsius)

	Smith	Sacramento	Feather	American	Merced	Kings
January		1.642	1.852	1.847	1.920	1.989
	1.495	1.637	1.783	1.809	1.872	1.918
February		1.339	1.524	1.528	1.411	1.301
	1.299	1.337	1.459	1.500	1.415	1.310
March		1.852	1.990	1.892	1.787	1.714
	1.653	1.840	1.913	1.856	1.741	1.650
April		1.498	1.477	1.396	1.284	1.197
	1.384	1.492	1.461	1.397	1.288	1.206
May		0.791	0.697	0.735	0.651	0.523
	0.963	0.796	0.722	0.753	0.705	0.607
June		1.403	1.359	1.304	1.281	1.347
	1.357	1.391	1.313	1.285	1.263	1.310
July		1.870	2.028	1.947	1.849	1.867
	1.626	1.861	1.976	1.919	1.801	1.794
August		1.294	1.245	1.224	1.213	1.184
	1.308	1.288	1.218	1.213	1.206	1.176
September		1.775	1.868	1.806	1.861	2.006
	1.581	1.763	1.808	1.776	1.814	1.941
October		0.631	0.531	0.702	1.000	1.077
	0.988	0.649	0.577	0.722	1.040	1.143
November		0.739	0.724	0.820	0.962	1.002
	0.925	0.747	0.716	0.820	0.997	1.060
December		1.986	2.045	1.986	1.940	2.007
	1.865	1.978	1.993	1.962	1.910	1.952

Table A.2. Temperature shifts HadCM2 2050-2079 (degrees Celsius)

	Smith	Sacramento	Feather	American	Merced	Kings
January		2.323	2.607	2.666	2.779	2.808
	2.248	2.322	2.523	2.623	2.750	2.768
February		2.023	2.339	2.387	2.368	2.276
	1.982	2.021	2.231	2.336	2.353	2.259
March		2.136	2.246	2.242	2.253	2.170
	2.111	2.135	2.202	2.223	2.246	2.169
April		2.423	2.517	2.403	2.290	2.272
	2.176	2.413	2.475	2.389	2.267	2.240
May		1.459	1.325	1.380	1.281	1.057
	1.639	1.465	1.373	1.411	1.351	1.163
June		2.688	2.731	2.591	2.433	2.517
	2.457	2.675	2.690	2.569	2.380	2.419
July		3.196	3.333	3.152	2.921	2.955
	2.778	3.177	3.264	3.116	2.846	2.830
August		3.240	3.181	2.951	2.688	2.717
	2.911	3.216	3.114	2.921	2.623	2.617
September		3.177	3.218	3.080	2.975	3.103
	2.874	3.164	3.190	3.063	2.918	3.020
October		2.230	2.187	2.235	2.389	2.530
	2.373	2.237	2.201	2.240	2.394	2.541
November		2.160	2.337	2.415	2.561	2.627
	2.157	2.166	2.314	2.404	2.566	2.638
December		2.950	2.988	2.947	2.917	2.898
	2.847	2.940	2.931	2.922	2.898	2.868

Table A.3. Temperature shifts HadCM2 2080-2099 (degrees Celsius)

	Smith	Sacramento	Feather	American	Merced	Kings
January		4.235	4.701	4.647	4.661	4.675
	3.841	4.216	4.523	4.558	4.569	4.543
February		2.964	3.266	3.294	3.221	3.054
	2.900	2.960	3.159	3.247	3.218	3.065
March		2.987	3.106	3.066	3.001	2.794
	2.904	2.978	3.026	3.034	2.992	2.797
April		3.667	3.858	3.730	3.611	3.489
	3.261	3.650	3.785	3.700	3.570	3.445
May		2.257	2.095	2.172	2.084	1.850
	2.472	2.265	2.160	2.212	2.173	1.986
June		3.528	3.542	3.409	3.281	3.318
	3.294	3.508	3.475	3.378	3.233	3.227
July		4.325	4.530	4.325	4.057	4.116
	3.862	4.310	4.471	4.293	3.973	3.982
August		4.330	4.285	4.075	3.897	3.996
	4.090	4.309	4.212	4.037	3.812	3.871
September		3.915	4.005	3.937	4.024	4.293
	3.759	3.909	3.960	3.907	3.955	4.199
October		2.497	2.362	2.534	2.970	3.167
	2.870	2.505	2.369	2.535	2.994	3.212
November		2.369	2.178	2.272	2.357	2.283
	2.666	2.374	2.204	2.297	2.440	2.420
December		3.812	4.013	4.005	4.004	3.959
	3.639	3.802	3.928	3.966	3.977	3.925

Table A.4. Temperature shifts PCM 2010-2039 (degrees Celsius)

	Smith	Sacramento	Feather	American	Merced	Kings
January		-0.078	0.081	0.111	0.163	0.201
	-0.141	-0.075	0.060	0.097	0.160	0.187
February		0.250	0.395	0.415	0.486	0.520
	0.146	0.255	0.371	0.392	0.478	0.490
March		0.162	0.188	0.264	0.406	0.467
	0.169	0.155	0.216	0.287	0.405	0.466
April		0.309	0.325	0.299	0.270	0.345
	0.281	0.310	0.313	0.280	0.260	0.309
May		0.165	0.116	0.058	-0.071	-0.112
	0.171	0.166	0.104	0.047	-0.072	-0.114
June		0.811	0.560	0.446	0.204	0.151
	0.844	0.810	0.588	0.458	0.212	0.171
July		0.749	0.710	0.654	0.498	0.441
	0.687	0.751	0.713	0.650	0.502	0.450
August		0.754	0.727	0.656	0.603	0.659
	0.722	0.756	0.695	0.619	0.590	0.606
September		0.954	1.025	0.947	0.869	0.867
	0.842	0.963	0.974	0.896	0.849	0.811
October		1.201	1.248	1.209	1.122	1.072
	1.120	1.205	1.224	1.182	1.108	1.037
November		0.740	0.753	0.761	0.716	0.655
	0.745	0.739	0.757	0.768	0.719	0.664
December		0.156	0.167	0.150	0.145	0.191
	0.172	0.155	0.150	0.128	0.138	0.167

Table A.5. Temperature shifts PCM 2050-2079 (degrees Celsius)

	Smith	Sacramento	Feather	American	Merced	Kings
January		1.562	1.710	1.670	1.624	1.633
	1.488	1.568	1.649	1.622	1.615	1.609
February		1.691	1.742	1.712	1.727	1.769
	1.654	1.696	1.708	1.681	1.718	1.743
March		1.151	1.176	1.196	1.254	1.334
	1.150	1.147	1.188	1.197	1.250	1.324
April		1.101	1.196	1.239	1.366	1.498
	1.055	1.101	1.192	1.226	1.353	1.450
May		1.341	1.330	1.240	1.006	0.903
	1.294	1.343	1.304	1.213	1.001	0.890
June		1.572	1.501	1.400	1.241	1.286
	1.516	1.576	1.492	1.378	1.235	1.257
July		2.242	2.434	2.335	2.192	2.251
	1.952	2.254	2.367	2.257	2.167	2.164
August		2.030	2.129	1.996	1.799	1.808
	1.843	2.037	2.057	1.921	1.778	1.738
September		1.967	2.078	2.037	2.080	2.128
	1.871	1.972	2.006	1.960	2.043	2.021
October		1.855	1.956	1.939	1.905	1.856
	1.757	1.861	1.926	1.912	1.891	1.830
November		1.731	1.779	1.835	1.892	1.878
	1.714	1.731	1.799	1.855	1.896	1.889
December		0.914	0.886	0.866	0.851	0.883
	0.996	0.913	0.868	0.853	0.851	0.885

Table A.6. Temperature shifts PCM 2080-2099 (degrees Celsius)

	Smith	Sacramento	Feather	American	Merced	Kings
January		2.259	2.455	2.350	2.194	2.219
	2.099	2.269	2.362	2.275	2.182	2.184
February		2.201	2.251	2.236	2.277	2.308
	2.162	2.206	2.220	2.208	2.269	2.287
March		2.442	2.505	2.547	2.652	2.730
	2.354	2.441	2.519	2.554	2.648	2.722
April		1.693	1.713	1.782	2.006	2.203
	1.732	1.690	1.718	1.775	1.989	2.138
May		2.384	2.584	2.509	2.384	2.358
	2.160	2.392	2.513	2.432	2.359	2.286
June		2.497	2.589	2.474	2.337	2.424
	2.316	2.508	2.530	2.408	2.315	2.348
July		2.728	2.920	2.820	2.725	2.862
	2.477	2.738	2.839	2.732	2.694	2.753
August		2.351	2.450	2.331	2.198	2.272
	2.181	2.356	2.381	2.257	2.174	2.181
September		2.717	2.760	2.660	2.607	2.678
	2.580	2.724	2.695	2.584	2.573	2.567
October		2.491	2.513	2.468	2.402	2.400
	2.418	2.493	2.490	2.435	2.385	2.357
November		2.935	2.955	2.975	2.938	2.910
	2.877	2.937	2.974	2.998	2.947	2.937
December		1.782	1.784	1.768	1.726	1.754
	1.822	1.778	1.776	1.759	1.728	1.764

Appendix VIII — Attachment B

Precipitation Ratios

Precipitation ratios for upper (gray rows) and lower (clear rows) sub-basins for the six study watersheds are provided. Tables B.1 to B.3 show the representative precipitation ratios for the HadCM2 scenario at time periods 2010-2039, 2050-2079, and 2080-2099, respectively.

Tables B.4 to B.6 show the representative precipitation ratios for the PCM scenario at time periods 2010-2039, 2050-2079, and 2080-2099, respectively.

Table B.1. Precipitation ratios HadCM2 2010-2039

	Smith	Sacramento	Feather	American	Merced	Kings
January		1.117	1.165	1.169	1.178	1.255
	1.087	1.121	1.170	1.171	1.181	1.252
February		1.166	1.211	1.255	1.341	1.449
	1.177	1.174	1.229	1.263	1.353	1.454
March		1.306	1.390	1.454	1.492	1.455
	1.283	1.313	1.413	1.466	1.524	1.492
April		1.177	1.264	1.301	1.366	1.382
	1.124	1.181	1.272	1.304	1.373	1.393
May		1.330	1.596	1.898	2.220	2.258
	1.278	1.349	1.665	1.927	2.292	2.335
June		1.075	1.107	1.061	1.282	1.350
	1.078	1.079	1.078	1.036	1.214	1.362
July		0.545	0.419	0.505	0.408	0.578
	0.738	0.551	0.445	0.602	0.411	0.673
August		0.826	0.839	0.837	0.763	0.861
	0.871	0.827	0.845	0.866	0.772	0.903
September		1.293	1.010	0.860	0.640	0.665
	1.425	1.288	1.019	0.870	0.608	0.645
October		1.248	1.351	1.315	1.281	1.262
	1.187	1.248	1.333	1.327	1.282	1.272
November		1.234	1.287	1.296	1.292	1.251
	1.181	1.232	1.277	1.291	1.292	1.253
December		1.089	1.044	1.013	0.956	0.954
	1.110	1.087	1.041	1.013	0.954	0.949

Table B.2. Precipitation ratios HadCM2 2050-2079

	Smith	Sacramento	Feather	American	Merced	Kings
January		1.224	1.267	1.249	1.171	1.172
	1.190	1.228	1.270	1.251	1.176	1.175
February		1.248	1.285	1.307	1.317	1.358
	1.257	1.253	1.295	1.312	1.326	1.361
March		1.444	1.603	1.734	1.857	1.829
	1.407	1.456	1.640	1.753	1.907	1.876
April		0.914	0.953	0.984	1.033	1.016
	0.893	0.915	0.955	0.985	1.046	1.034
May		1.279	1.614	1.925	2.246	2.228
	1.171	1.298	1.673	1.938	2.286	2.289
June		1.058	1.122	1.107	1.338	1.439
	1.018	1.054	1.083	1.093	1.266	1.449
July		0.572	0.392	0.391	0.351	0.613
	0.733	0.572	0.408	0.477	0.346	0.713
August		0.483	0.603	0.794	1.086	1.191
	0.533	0.479	0.565	0.778	1.123	1.267
September		1.003	1.003	0.956	0.768	0.700
	1.023	1.004	1.012	0.961	0.766	0.710
October		1.467	1.456	1.325	1.150	1.089
	1.446	1.465	1.423	1.327	1.134	1.075
November		1.084	1.169	1.216	1.314	1.415
	1.067	1.089	1.177	1.219	1.322	1.423
December		1.277	1.281	1.282	1.286	1.340
	1.292	1.278	1.281	1.282	1.289	1.334

Table B.3. Precipitation ratios HadCM2 2080-2099

	Smith	Sacramento	Feather	American	Merced	Kings
January		1.568	1.629	1.644	1.657	1.743
	1.551	1.576	1.641	1.648	1.663	1.741
February		1.526	1.702	1.801	1.917	2.032
	1.472	1.542	1.735	1.814	1.935	2.039
March		1.332	1.448	1.537	1.724	1.902
	1.320	1.347	1.491	1.556	1.747	1.917
April		0.986	1.017	1.039	1.084	1.126
	0.987	0.989	1.020	1.040	1.090	1.131
May		1.401	1.579	1.701	1.984	2.239
	1.281	1.412	1.613	1.698	1.971	2.239
June		1.109	1.264	1.314	1.736	2.252
	1.085	1.117	1.253	1.307	1.736	2.351
July		0.904	0.806	1.005	0.755	0.859
	1.054	0.913	0.870	1.191	0.792	0.914
August		0.639	0.887	1.161	1.333	1.434
	0.570	0.642	0.908	1.185	1.389	1.523
September		1.165	0.969	0.871	0.850	0.837
	1.291	1.162	0.961	0.873	0.796	0.831
October		1.628	1.636	1.465	1.181	1.103
	1.622	1.628	1.602	1.472	1.157	1.077
November		1.244	1.226	1.227	1.229	1.318
	1.279	1.248	1.241	1.236	1.236	1.320
December		1.377	1.468	1.529	1.641	1.776
	1.364	1.386	1.484	1.535	1.650	1.770

Table B.4. Precipitation ratios PCM 2010-2039

	Smith	Sacramento	Feather	American	Merced	Kings
January		0.842	0.869	0.874	0.905	0.930
	0.832	0.844	0.858	0.866	0.901	0.917
February		1.045	1.072	1.070	1.060	1.057
	1.023	1.047	1.067	1.065	1.059	1.054
March		1.003	0.972	0.942	0.866	0.818
	1.006	1.003	0.970	0.938	0.867	0.824
April		1.020	1.010	1.001	0.956	0.909
	1.026	1.020	1.012	1.003	0.958	0.917
May		1.107	1.151	1.232	1.268	1.176
	1.108	1.105	1.176	1.270	1.284	1.217
June		0.962	1.601	1.662	1.845	1.798
	0.594	0.994	1.470	1.524	1.812	1.744
July		1.469	1.194	1.323	1.361	1.074
	1.275	1.458	1.261	1.403	1.386	1.149
August		0.406	0.453	0.647	0.924	0.723
	0.470	0.405	0.456	0.692	0.955	0.772
September		0.868	0.777	0.834	0.883	0.825
	0.930	0.864	0.778	0.839	0.886	0.833
October		0.678	0.777	0.879	1.078	1.104
	0.701	0.680	0.770	0.888	1.079	1.115
November		0.966	0.996	1.014	1.073	1.140
	0.956	0.968	0.993	1.015	1.071	1.136
December		0.901	0.908	0.914	0.948	0.945
	0.906	0.902	0.898	0.904	0.943	0.936

Table B.5. Precipitation ratios PCM 2050-2079

	Smith	Sacramento	Feather	American	Merced	Kings
January		1.153	1.160	1.132	1.065	1.050
	1.129	1.155	1.151	1.124	1.065	1.047
February		1.022	1.070	1.079	1.094	1.104
	1.001	1.023	1.065	1.072	1.092	1.098
March		0.923	0.940	0.928	0.897	0.864
	0.906	0.925	0.929	0.919	0.897	0.867
April		0.877	0.824	0.773	0.670	0.640
	0.895	0.876	0.818	0.765	0.670	0.640
May		0.952	1.006	1.092	1.224	1.188
	0.967	0.952	1.014	1.113	1.229	1.208
June		1.429	1.600	1.571	1.525	1.595
	1.212	1.436	1.574	1.517	1.509	1.555
July		0.579	0.616	0.803	0.995	0.667
	0.481	0.574	0.633	0.871	1.016	0.737
August		0.262	0.298	0.462	0.622	0.431
	0.357	0.260	0.337	0.561	0.668	0.506
September		0.597	0.573	0.626	0.718	0.707
	0.650	0.597	0.581	0.645	0.721	0.711
October		0.761	0.886	0.949	1.068	1.098
	0.713	0.766	0.871	0.951	1.070	1.109
November		0.658	0.606	0.564	0.522	0.545
	0.693	0.659	0.596	0.555	0.522	0.541
December		0.778	0.778	0.786	0.814	0.805
	0.788	0.779	0.774	0.785	0.814	0.805

Table B.6. Precipitation ratios PCM 2080-2099

	Smith	Sacramento	Feather	American	Merced	Kings
January		0.847	0.854	0.837	0.822	0.845
	0.849	0.848	0.843	0.829	0.820	0.836
February		1.073	1.032	0.983	0.901	0.890
	1.092	1.073	1.020	0.972	0.900	0.886
March		0.774	0.752	0.722	0.690	0.694
	0.789	0.775	0.738	0.709	0.687	0.684
April		1.214	1.164	1.087	0.869	0.742
	1.200	1.214	1.161	1.080	0.875	0.763
May		0.638	0.675	0.753	0.765	0.591
	0.655	0.640	0.694	0.796	0.785	0.650
June		0.849	1.058	1.101	1.129	0.937
	0.653	0.862	1.047	1.095	1.133	0.963
July		0.654	0.329	0.575	0.850	0.707
	0.706	0.629	0.425	0.684	0.875	0.753
August		0.435	0.119	0.292	0.601	0.448
	0.581	0.413	0.162	0.364	0.629	0.500
September		0.531	0.437	0.451	0.509	0.495
	0.607	0.529	0.444	0.464	0.510	0.494
October		0.444	0.568	0.737	1.037	1.014
	0.469	0.445	0.573	0.766	1.041	1.037
November		0.625	0.542	0.500	0.483	0.528
	0.687	0.624	0.531	0.488	0.479	0.512
December		0.876	0.890	0.905	0.972	1.003
	0.885	0.877	0.877	0.895	0.967	0.989

Appendix VIII — Attachment C

Incrementally Forced Streamflow Sensitivity Values

Streamflow ratios for each the six study watersheds are provided. Table C.1 corresponds to 1.5°C increase and 0.0% precipitation change and Table C.2 corresponds to 1.5°C increase and 9.0% precipitation change. Table C.3 corresponds to 3.0°C increase and 0.0% precipitation change and Table C.4 corresponds to 3.0°C increase and 18.0% precipitation change. Table C.5 corresponds to 5.0°C increase and 0.0% precipitation change and Table C.6 corresponds to 5.0°C increase and 30.0% precipitation change.

Table C.1. Mean-monthly streamflow ratios for 1.5°C T,^a 0% P^b

	Smith	Sacramento	Feather	American	Merced	Kings
January	1.039	1.234	1.352	1.163	2.160	1.181
February	0.983	1.120	1.262	1.181	1.932	1.168
March	0.951	1.088	1.188	1.181	1.650	1.310
April	0.960	0.973	0.915	1.020	1.329	1.381
May	0.981	0.734	0.622	0.677	0.899	1.047
June	0.988	0.625	0.542	0.483	0.701	0.762
July	0.989	0.759	0.758	0.508	0.548	0.687
August	0.989	0.861	0.862	0.798	0.507	0.751
September	0.992	0.862	0.886	0.912	0.595	0.871
October	0.997	0.903	0.937	0.966	0.864	0.865
November	1.003	1.096	1.095	1.086	1.356	0.983
December	1.034	1.213	1.278	1.144	1.802	1.123

a. T: temperature.

b. P: precipitation.

Table C.2. Mean-monthly streamflow ratios for 1.5°C T,^a 9% P^b

	Smith	Sacramento	Feather	American	Merced	Kings
January	1.148	1.408	1.544	1.360	2.567	1.367
February	1.079	1.265	1.416	1.341	2.145	1.319
March	1.047	1.208	1.336	1.334	1.867	1.469
April	1.050	1.075	1.044	1.134	1.458	1.514
May	1.072	0.827	0.719	0.778	1.022	1.181
June	1.068	0.705	0.636	0.587	0.835	0.886
July	1.037	0.831	0.820	0.605	0.677	0.810
August	1.044	0.935	0.931	0.871	0.628	0.860
September	1.091	0.955	0.958	0.986	0.740	0.955
October	1.147	1.029	1.044	1.155	1.065	0.965
November	1.178	1.299	1.307	1.343	1.749	1.132
December	1.166	1.419	1.503	1.365	2.152	1.339

a. T: temperature.

b. P: precipitation.

Table C.3. Mean-monthly streamflow ratios for 3.0°C T,^a 0% P^b

	Smith	Sacramento	Feather	American	Merced	Kings
January	1.038	1.394	1.605	1.316	3.850	1.428
February	0.971	1.255	1.459	1.328	3.146	1.497
March	0.944	1.149	1.225	1.251	2.435	1.851
April	0.959	0.862	0.742	0.928	1.437	1.693
May	0.980	0.504	0.360	0.401	0.681	0.916
June	0.988	0.442	0.383	0.239	0.409	0.516
July	0.988	0.633	0.672	0.352	0.255	0.470
August	0.989	0.782	0.769	0.704	0.264	0.589
September	0.992	0.783	0.804	0.860	0.343	0.744
October	0.997	0.859	0.887	0.945	0.789	0.786
November	1.003	1.163	1.136	1.160	1.617	0.937
December	1.049	1.430	1.480	1.280	2.894	1.295

a. T: temperature.

b. P: precipitation.

Table C.4. Mean-monthly streamflow ratios for 3.0°C T,^a 18% P^b

	Smith	Sacramento	Feather	American	Merced	Kings
January	1.252	1.780	2.081	1.754	5.023	1.908
February	1.163	1.565	1.830	1.687	3.874	1.872
March	1.133	1.412	1.543	1.595	2.964	2.242
April	1.135	1.055	0.949	1.154	1.753	2.049
May	1.163	0.635	0.462	0.545	0.901	1.169
June	1.144	0.528	0.453	0.335	0.584	0.701
July	1.083	0.730	0.762	0.428	0.393	0.633
August	1.096	0.899	0.881	0.807	0.378	0.729
September	1.192	0.914	0.926	1.006	0.550	0.889
October	1.314	1.098	1.097	1.370	1.250	0.933
November	1.357	1.605	1.610	1.737	2.668	1.328
December	1.317	1.911	2.018	1.767	4.037	1.851

a. T: temperature.

b. P: precipitation.

Table C.5. Mean-monthly streamflow ratios for 5.0°C T,^a 0% P^b

	Smith	Sacramento	Feather	American	Merced	Kings
January	1.038	1.535	1.755	1.430	6.372	2.008
February	0.968	1.323	1.517	1.402	4.804	2.163
March	0.944	1.108	1.187	1.208	3.156	2.679
April	0.959	0.750	0.602	0.816	1.233	1.756
May	0.980	0.389	0.256	0.266	0.370	0.585
June	0.988	0.380	0.334	0.182	0.139	0.288
July	0.988	0.595	0.626	0.322	0.088	0.285
August	0.989	0.742	0.716	0.671	0.111	0.478
September	0.992	0.751	0.756	0.825	0.153	0.652
October	0.997	0.838	0.856	0.925	0.718	0.698
November	1.003	1.246	1.160	1.224	2.012	0.925
December	1.051	1.612	1.597	1.344	4.277	1.689

a. T: temperature.

b. P: precipitation.

Table C.6. Mean-monthly streamflow ratios for 5.0°C T,^a 30% P^b

	Smith	Sacramento	Feather	American	Merced	Kings
January	1.390	2.243	2.639	2.211	9.455	3.079
February	1.285	1.879	2.173	2.065	6.726	3.019
March	1.257	1.542	1.712	1.792	4.283	3.634
April	1.251	1.017	0.868	1.154	1.781	2.434
May	1.288	0.529	0.333	0.400	0.582	0.897
June	1.242	0.472	0.411	0.268	0.286	0.443
July	1.146	0.715	0.753	0.406	0.165	0.416
August	1.166	0.907	0.873	0.809	0.204	0.581
September	1.332	0.954	0.936	1.057	0.381	0.769
October	1.565	1.240	1.198	1.672	1.497	0.844
November	1.605	2.069	2.022	2.324	4.415	1.629
December	1.497	2.521	2.622	2.243	7.343	2.978

a. T: temperature.

b. P: precipitation.

Appendix VIII — Attachment D

GCM-Forced Streamflow Sensitivity Values

Streamflow ratios for each the six study watersheds are provided. Tables D.1 to D.3 show the representative streamflow ratios for the HadCM2 scenario at 2010-2039, 2050-2079, and 2080-2099, respectively. Tables D.4 to D.6 show the representative streamflow ratios for the PCM scenario at 2010-2039, 2050-2079, and 2080-2099, respectively.

Table D.1. Mean-monthly streamflow ratios for HadCM2 2010-2039

	Smith	Sacramento	Feather	American	Merced	Kings
January	1.149	1.518	1.812	1.568	3.350	1.679
February	1.152	1.356	1.605	1.605	2.499	1.726
March	1.231	1.466	1.760	1.864	2.287	2.014
April	1.112	1.181	1.231	1.363	1.642	1.785
May	1.228	0.931	0.831	1.042	1.261	1.406
June	1.135	0.789	0.744	0.823	1.177	1.320
July	1.059	0.881	0.887	0.719	1.055	1.274
August	1.041	0.994	1.004	0.999	0.941	1.208
September	1.363	1.064	1.018	1.097	0.835	1.070
October	1.388	1.202	1.269	1.495	1.237	1.101
November	1.371	1.498	1.696	1.884	2.077	1.400
December	1.230	1.621	1.738	1.460	2.449	1.500

Table D.2. Mean-monthly streamflow ratios for HadCM2 2050-2079

	Smith	Sacramento	Feather	American	Merced	Kings
January	1.269	1.794	2.227	1.893	4.965	2.055
February	1.238	1.550	1.916	1.836	3.601	1.982
March	1.350	1.642	1.989	2.269	2.960	2.665
April	0.956	1.059	1.117	1.248	1.863	2.137
May	1.095	0.785	0.674	0.863	1.212	1.411
June	1.062	0.654	0.603	0.634	1.057	1.226
July	1.016	0.805	0.847	0.578	0.830	1.116
August	0.951	0.933	0.966	0.933	0.710	1.092
September	0.984	0.915	0.988	1.076	0.709	1.040
October	1.672	1.388	1.365	1.628	1.252	1.066
November	1.243	1.475	1.700	1.874	3.045	1.668
December	1.427	2.064	2.277	2.003	4.467	2.352

Table D.3. Mean-monthly streamflow ratios for HadCM2 2080-2099

	Smith	Sacramento	Feather	American	Merced	Kings
January	1.658	2.680	3.426	2.920	10.806	3.842
February	1.477	2.122	2.717	2.805	6.129	3.468
March	1.294	1.663	2.048	2.240	3.881	3.483
April	1.016	1.031	1.030	1.240	2.307	2.888
May	1.199	0.688	0.509	0.663	1.224	1.674
June	1.128	0.558	0.520	0.458	0.996	1.401
July	1.066	0.762	0.825	0.488	0.715	1.291
August	0.987	0.932	0.950	0.891	0.607	1.250
September	1.202	0.945	0.967	1.042	0.664	1.138
October	2.159	1.589	1.536	1.918	1.362	1.153
November	1.649	1.847	1.901	1.974	2.594	1.584
December	1.578	2.570	2.974	2.669	7.373	3.391

Table D.4. Mean-monthly streamflow ratios for PCM 2010-2039

	Smith	Sacramento	Feather	American	Merced	Kings
January	0.814	0.793	0.853	0.816	1.092	0.978
February	0.981	0.966	1.032	1.052	1.231	1.080
March	0.991	0.977	0.980	0.974	1.167	0.972
April	1.007	0.981	0.952	0.983	1.054	1.054
May	1.068	0.919	0.886	0.919	0.931	0.937
June	0.907	0.875	0.906	0.940	0.964	0.924
July	0.986	0.927	0.883	0.946	0.910	0.906
August	0.911	0.920	0.929	0.964	0.881	0.903
September	0.895	0.907	0.923	0.978	0.835	0.925
October	0.650	0.750	0.850	0.860	1.077	0.927
November	0.819	0.908	0.969	0.995	1.378	1.082
December	0.865	0.851	0.907	0.891	1.179	1.048

Table D.5. Mean-monthly streamflow ratios for PCM 2050-2079

	Smith	Sacramento	Feather	American	Merced	Kings
January	1.079	1.181	1.267	1.018	1.429	0.964
February	0.989	1.098	1.281	1.185	1.628	1.136
March	0.869	0.964	1.045	1.030	1.294	1.104
April	0.864	0.846	0.770	0.838	1.073	1.132
May	0.924	0.680	0.584	0.626	0.770	0.847
June	1.034	0.626	0.567	0.511	0.653	0.683
July	0.969	0.717	0.719	0.490	0.518	0.641
August	0.891	0.786	0.794	0.756	0.443	0.683
September	0.730	0.739	0.794	0.846	0.458	0.781
October	0.612	0.681	0.818	0.811	0.852	0.805
November	0.492	0.583	0.509	0.391	0.511	0.746
December	0.671	0.668	0.641	0.547	0.780	0.624

Table D.6. Mean-monthly streamflow ratios for PCM 2080-2099

	Smith	Sacramento	Feather	American	Merced	Kings
January	0.825	0.915	1.006	0.745	1.519	0.859
February	1.006	1.077	1.172	1.020	1.759	0.979
March	0.770	0.882	0.888	0.843	1.484	1.173
April	1.061	0.889	0.686	0.820	1.013	1.162
May	0.797	0.493	0.388	0.425	0.566	0.690
June	0.768	0.416	0.358	0.247	0.365	0.415
July	0.883	0.578	0.591	0.318	0.232	0.387
August	0.847	0.688	0.654	0.618	0.228	0.494
September	0.680	0.656	0.665	0.720	0.227	0.633
October	0.393	0.531	0.599	0.582	0.633	0.674
November	0.420	0.472	0.384	0.268	0.394	0.623
December	0.730	0.762	0.702	0.619	1.126	0.672